

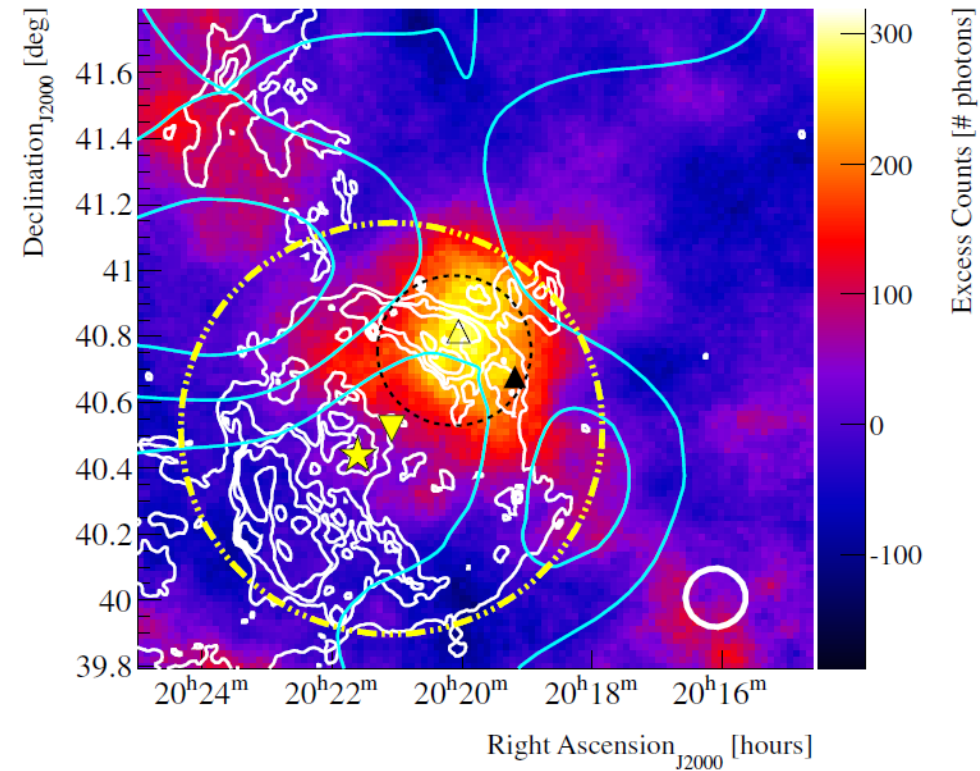
# Exploring the Gamma-Ray Emission From Young Core-Collapse Supernovae, and their Detectability with the Cherenkov Telescope Array

*Vikram Dwarkadas* (University of Chicago)

(In collaboration with Alexandre Marcowith (University Montpellier), Pierre Cristofari (Paris Observatory), Matthieu Renaud (University Montpellier), Vincent Tatischeff (University Paris-Sud), Fabio Acero (CNRS), Justine Devine (CNRS, Montpellier) plus many others)

# Gamma-rays from SNe

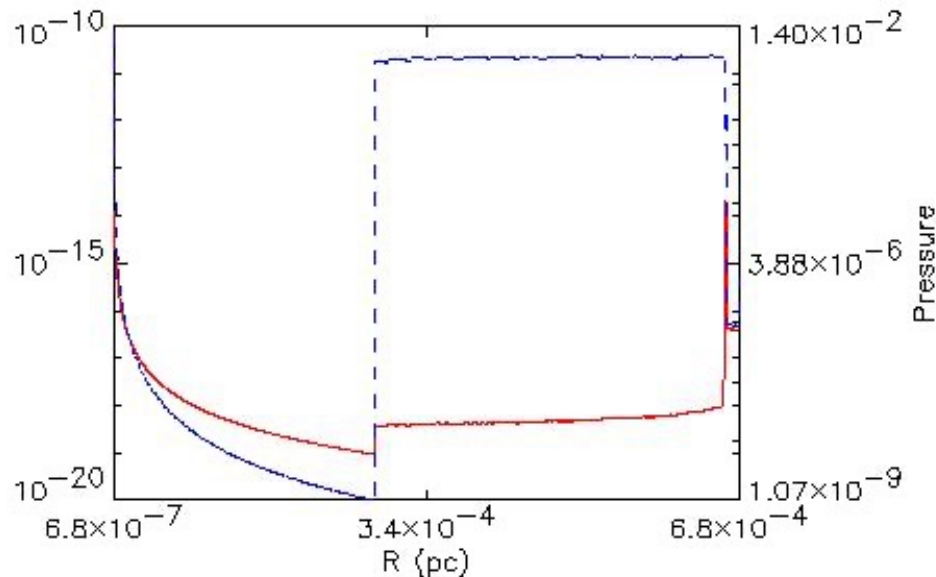
- We have started a large project to study various aspects of gamma-ray emission from SNe.
- We look at the **amplification** of the magnetic field, **maximum energy** via various processes, and **absorption** of the emission in young SNe.
- The goal is to **understand particle acceleration in young SNe**, and help to set the **observing agenda for the Cerenkov Telescope Array (CTA)** with regards to young SNe.



# Young Core-Collapse SNe

# Core-Collapse Supernovae (SNe)

- Arise from Massive Stars
- These stars have strong winds throughout their lifetimes
- If the wind mass-loss rate  $\dot{M}$  and the wind velocity  $v_w$  are constant, then the wind density  $\rho_w = \dot{M} / (4\pi r^2 v_w) \propto r^{-2}$ . In general  $\rho_w \propto r^{-s}$
- ➡ Density is maximum at small radius, i.e. close in to the star.



Red=Density

Blue=Pressure

Density and pressure structure around a star, from a simulation of a stellar wind interacting with the Interstellar medium. Density is very high close in to the star.

# Shock Dynamics

- Assume SN ejecta and circumstellar medium evolve as power-law with time.
- Shock radius  $\rightarrow$  self-similar solution (Chevalier 82):

$$R_{sh} \propto t^m$$

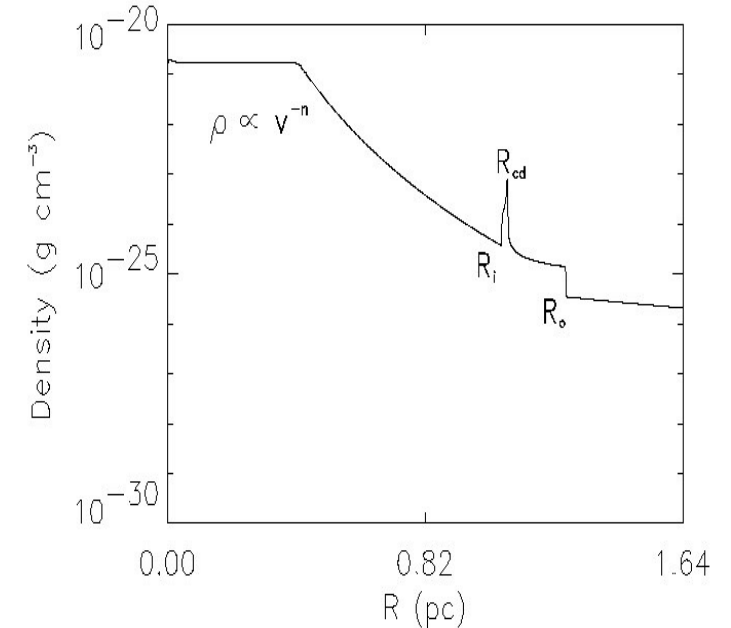
- If we start from initial time  $t_0$  where shock radius is  $R_0$  then

$$R_{sh}(t) = R_0 \left[ \frac{t}{t_0} \right]^m, \quad V_{sh}(t) = \frac{R_0 m}{t_0} \times \left( \frac{t}{t_0} \right)^{m-1}$$

Wind density:

$$\rho_{CSM}(t) = \rho_0 \left[ \frac{R_{sh}(t)}{R_0} \right]^{-s} = \rho_0 \left[ \frac{t}{t_0} \right]^{-ms}, \quad s=2 \text{ for steady wind}$$

$$\rho_0 = \frac{\dot{M}(R_0)}{4\pi v_w(R_0) R_0^2} \cong 1.3 m_p n_H$$



# Magnetic Field Strength

- Magnetic field strength at stellar surface, obtained by balance between magnetic energy density and kinetic energy density:

$$B_{eq,0} = \left[ \frac{2.5 \times 10^{13}}{R_0} G \right] \dot{M}_{-5}^{1/2} V_w^{1/2}$$

CSM magnetic field proportional to  $B_{eq,0}$

$$B_w(t) \cong \varpi B_{eq,0} \left[ \frac{t}{t_0} \right]^{\frac{-ms}{2}}, \text{ where } \varpi = B_w(t_0)/B_{eq,0} \sim 0.1-10.$$

# Acceleration Model

- We adopt a model based on the theory of Diffusive Shock Acceleration (DSA).
- Timescale to advect frozen CR-magnetized fluid to shock front is:

$$T_{adv,u} = \frac{\kappa_u}{v_{sh}^2}$$

Parallel shocks:  $\kappa_u = \kappa_{II} = \frac{\eta R_L v}{3}$ , where  $R_L =$  Larmor radius  $\cong E/eB_w$

Writing  $R_L = 3.3 \times 10^{12} E_{PeV} B_{w,G}^{-1}$  cm, we get

$$T_{adv,u,P} \cong \left[ \frac{1.3 \times 10^9 \eta_P R_{0,cm}}{V_{0,\frac{cm}{s}}^2 \varpi} \right] \times \frac{E_{PeV}}{\dot{M}_{-5}^{\frac{1}{2}} v_{w,10}^{\frac{1}{2}}} \left( \frac{t}{t_0} \right)^{2(1-m)+ms/2}$$

# Acceleration timescale

$$T_{acc,P} = g(r)T_{adv,u,P} = g(r)\frac{\kappa_u}{v_{sh}^2}$$

Where  $g(r) = \frac{3r}{r-1} \times \left(1 + \frac{\kappa_d r}{\kappa_u}\right)$  depends on shock compression ratio  $r$  and ratio of downstream to upstream coefficients.

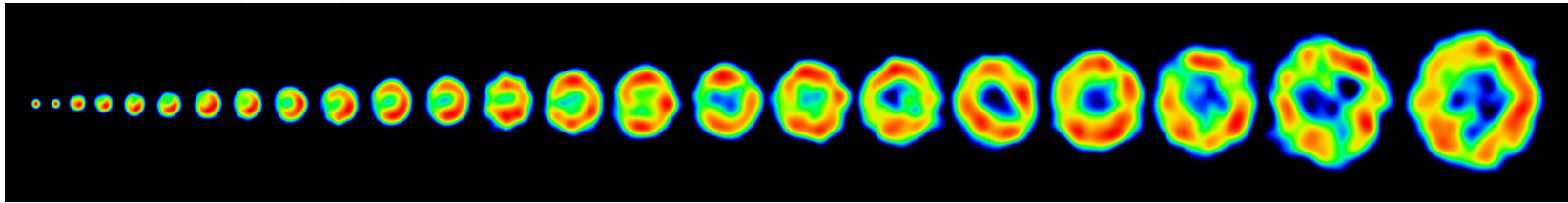
Ratio  $\frac{\kappa_d}{\kappa_u} = r_B^{-1}$ ,  $r_B = \frac{B_d}{B_u}$  is ratio of magnetic fields in postshock region.

For parallel shock,  $r_B \cong 1$  and  $g(r) = 3r(r+1)/(r-1)$



# Observed Magnetic Field Strength

Magnetic fields in Young SNe difficult to interpret. One usually gets synchrotron radio emission, and from there needs to deduce the magnetic field depending on the volume and other unknown parameters. **But almost always seems much higher than the interstellar field by orders of magnitude.**

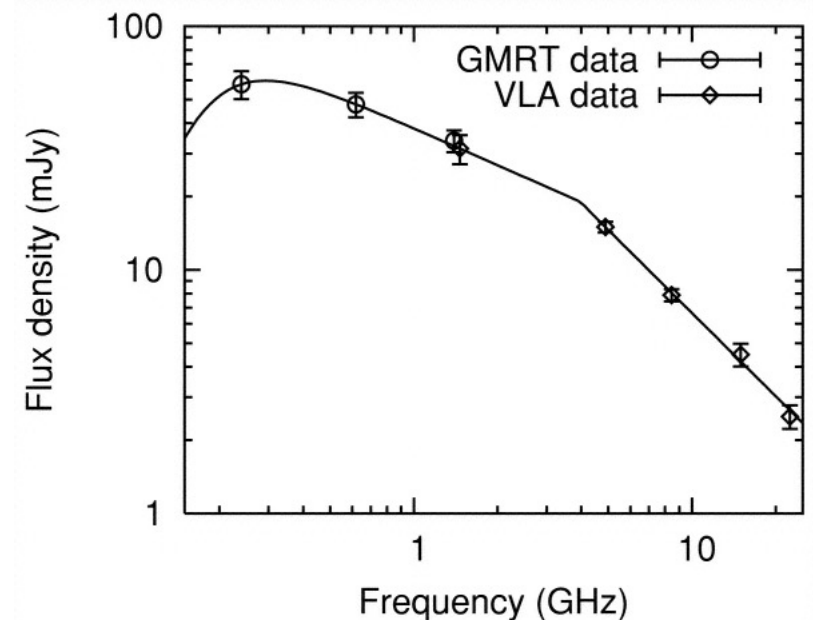


Chandra et al 2004, ApJ, 604, L97

Magnetic field for SN 1993J can be deduced from synchrotron break in the spectrum to be 0.33G, at 3200 d.

Comparable to field deduced by Fransson & Bjornsson 1998 from analysis of radio emission.

The field is much larger than the interstellar magnetic field.



# Cosmic-Ray Driven Instabilities

- These operate on the forward shock and generate magnetic field fluctuations necessary for the DSA process to operate efficiently.

## 1. Bell Non-resonant Instability (Bell 2001, 2004)

- Currents produced by the streaming of CRs ahead of the shock front.
- CR streaming induces a return current in the background plasma.
- Triggers magnetic fluctuations at scales  $l \ll R_L$
- Is non-resonant, and can be treated using modified MHD code.
- The minimum growth time-scale (corresponding to maximal growth rate)

$$T_{min,NRS} \cong \left[ \frac{2.2 \times 10^{18} R_0}{V_0^3} \right] \frac{\Phi_{14}}{\xi_{CR,0.05}} E_{PeV} \times \dot{M}_{-5}^{-1/2} V_{w,10}^{1/2} \left( \frac{t}{t_0} \right)^{2(1-m)+(ms)/2}$$


Note: The acceleration time is inversely proportional to  $V_{sh}^3$ , thus it is lowest at the highest velocities, i.e. just after explosion. Since  $m < 1$ , it is increasing with time.

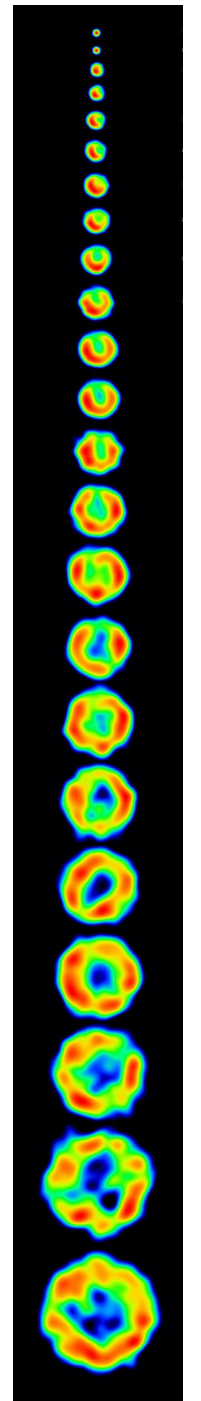
Where  $\Phi_{14} \equiv \frac{\ln\left(\frac{E_{max}}{m_p c^2}\right)}{14}$ ,  $\xi_{CR}$  is fraction of shock ram pressure imparted to CRs

# Cosmic-ray Driven Instabilities

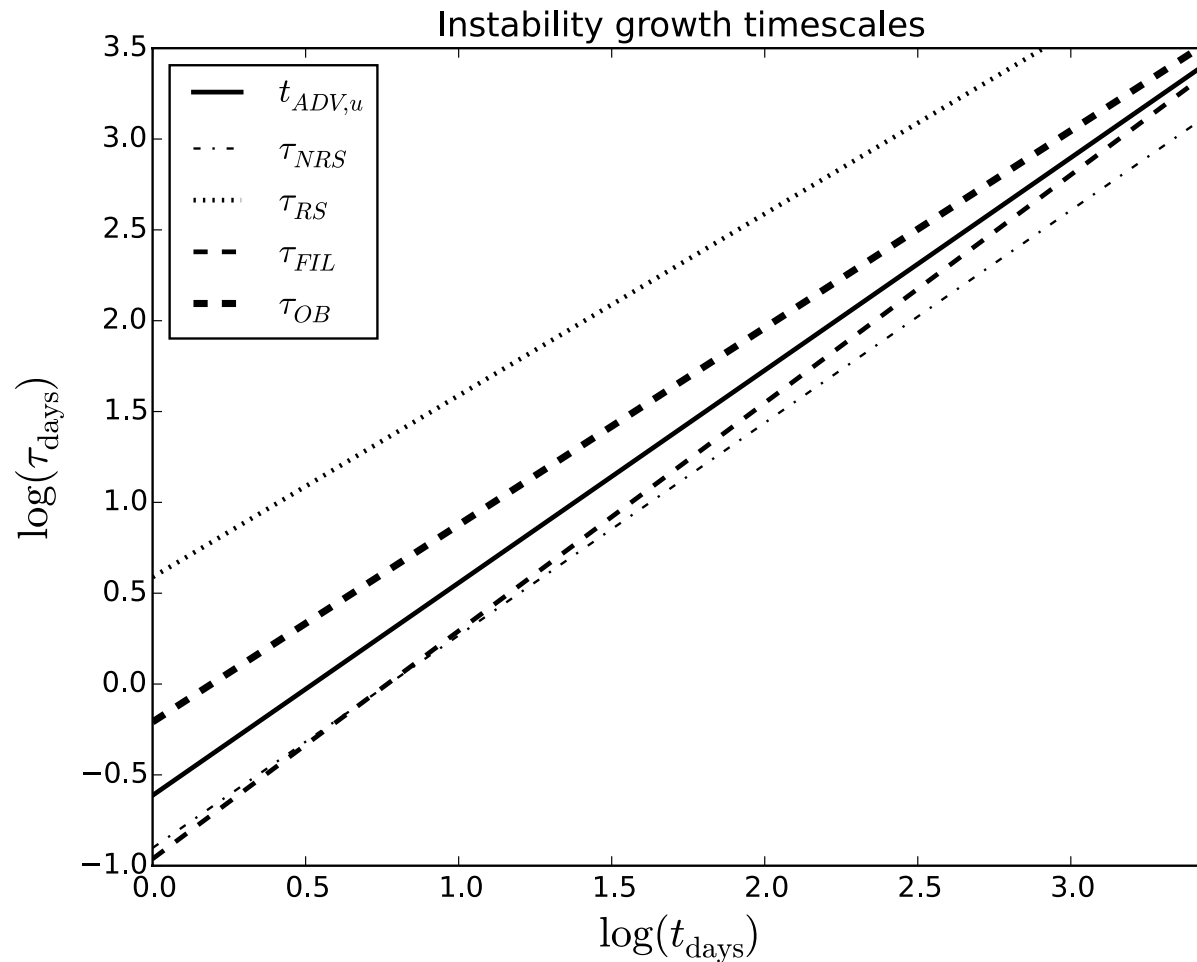
- **Resonant streaming Instability:** Streaming of Cosmic Rays faster than the local Alfvén speed produces long-wavelength modes at scales  $l \sim R_L$  (Amato & Blasi 2009)
- **Filamentation Instability:** Reville & Bell (2012) demonstrate that CRs form filamentary structures in the precursors of SNR shocks due to their self-generated magnetic fields. The filamentation results in growth of a long-wavelength instability.
- **Instabilities generating long oblique modes:** Bykov et al. (2011) show that presence of turbulence with scales shorter than the CR gyroradius enhances growth of modes longer than gyroradius for particular polarizations.

# Application - SN 1993J

- Type IIb SN - possible RSG progenitor (Chevalier & Oishi 2003)
- Occurred in M81 – Distance 3.6 Mpc
- VLBI observations provide information on expansion, radius and velocity
- Mass-loss rate  $4 \times 10^{-5} M_{\odot} \text{ yr}^{-1}$
- Tatischeff (2009):  $\langle B \rangle \approx [2.4 \pm 1G] \times (t / 100d)^{-1.16 \pm 0.2}$
- Compare with equipartition magnetic field:
$$B_{eq} \cong [2.5mG] \times M_{-5}^{1/2} u_{w,10}^{1/2} r_{16}^{-1}$$
-  Magnetic field amplified substantially
- Chandra et al 2004:  $B_{eq} \sim 38 \text{ mG}$  around day 3200



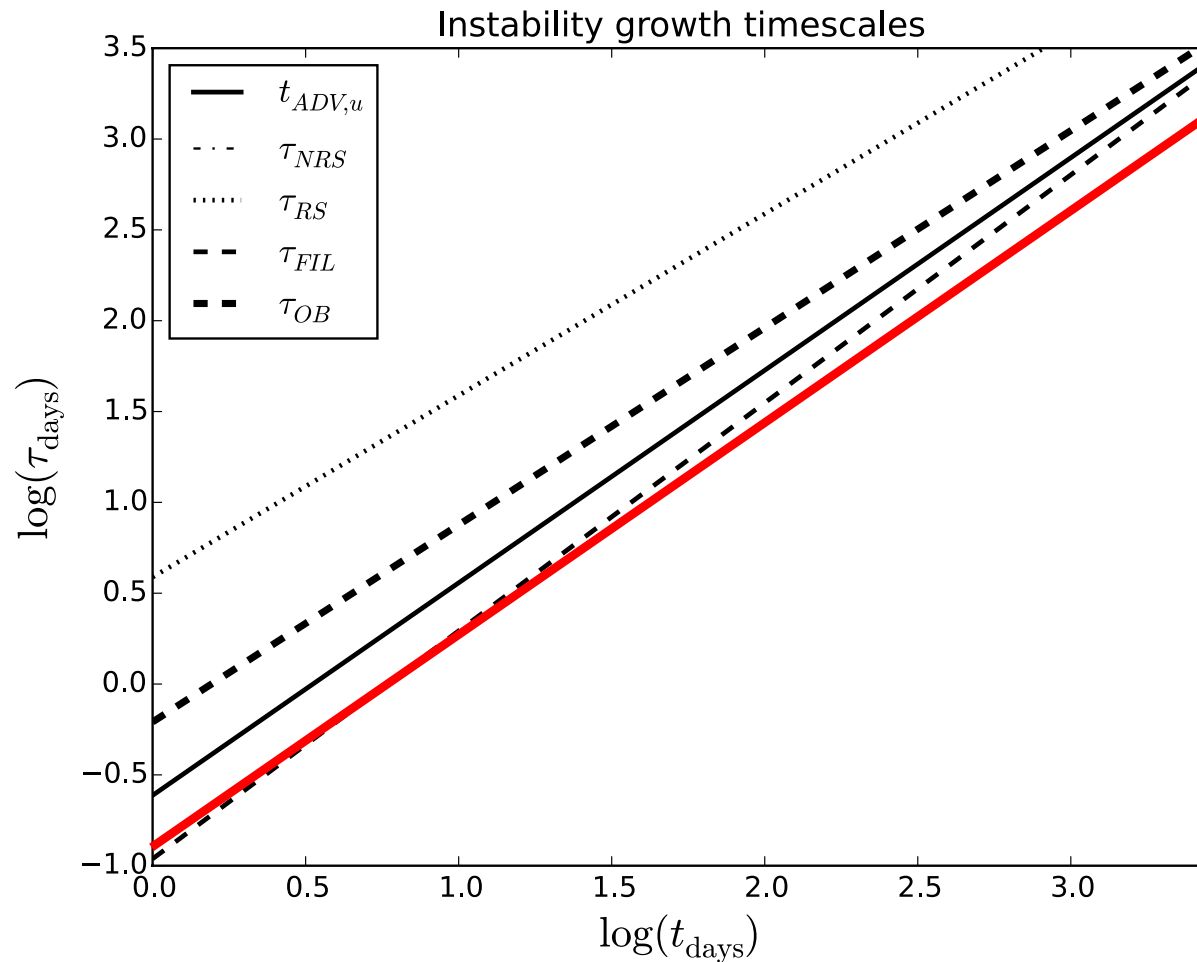
# Instability Growth timescales



Main instability growth timescales as a function of the time in days for the fiducial case SN 1993. We have assumed  $\eta = \varpi = 1$ ,  $E = 1$  PeV,  $\phi = 14$ ,  $\xi_{\text{CR}} = 0.05$ .

(Marcowith, VVD, et al. 2018, MNRAS, 479, 4470.)

# Instability Growth timescales



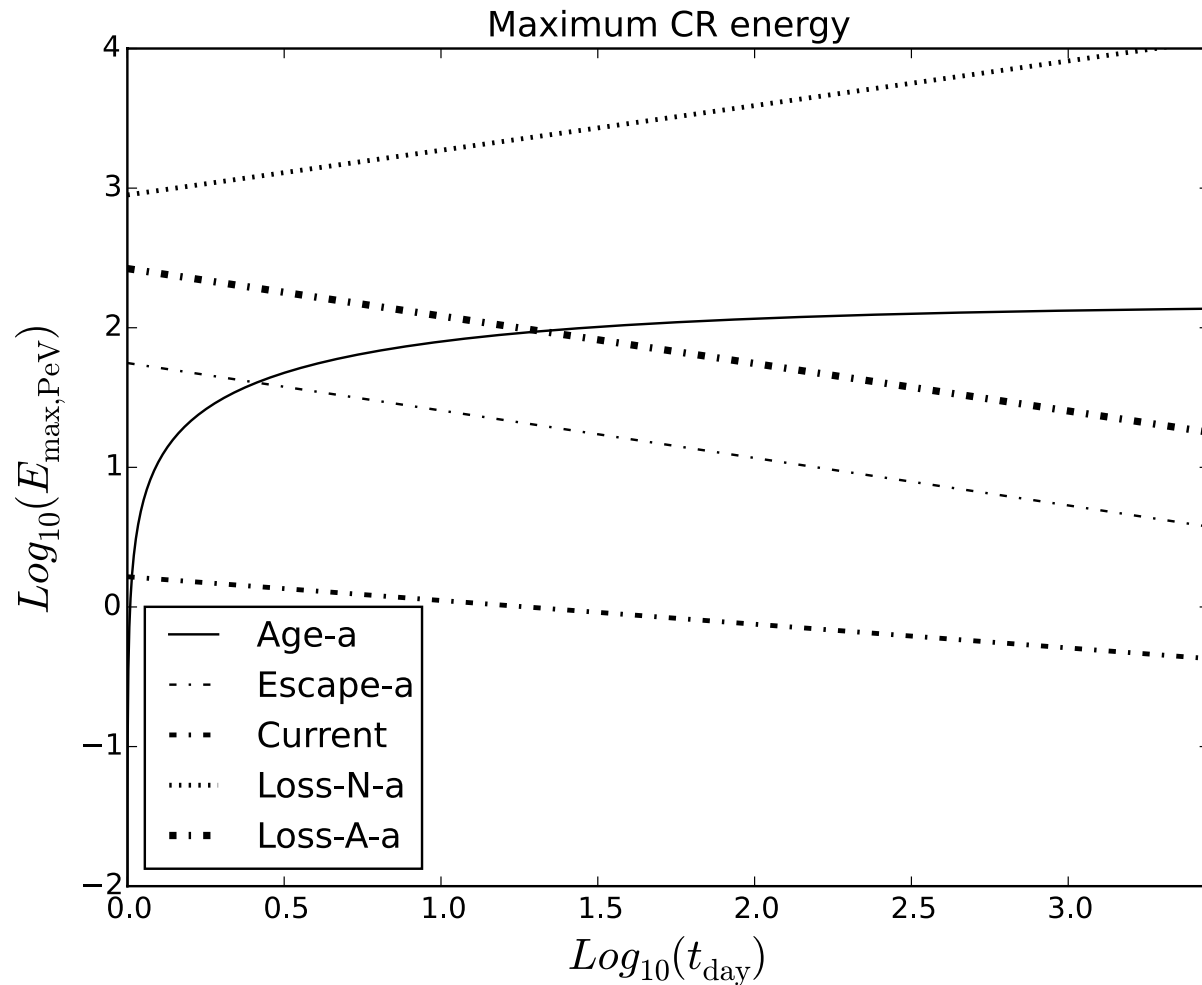
Main instability growth timescales as a function of the time in days for the fiducial case SN 1993. We have assumed  $\eta = \varpi = 1$ ,  $E = 1$  PeV,  $\phi = 14$ ,  $\xi_{\text{CR}} = 0.05$ .

(Marcowith, VVD et al 2018, MNRAS, 479, 4470)

# Maximum Cosmic-Ray Energies

- ❖ **Age limitation** -  $T_{acc} = \left(\frac{1}{E} \frac{dE}{dt}\right)^{-1}$  -acceleration limited by shock age
- ❖ **Geometrical losses** due to finite spatial extent of the shock
- ❖ **Current-driven maximum energy**: If NRS instability operates,  $\frac{t}{T_{min.NRS}} = N, N \in [1, \ln A]$ , where A corresponds to amplification of magnetic field by factor A.
- ❖ **Nuclear Interaction losses**: High-energy CRs interact with ambient material via p-p interactions. (Mainly relevant for PeV energies).
- ❖ **Adiabatic Losses**: CRs suffer from adiabatic losses in rapidly expanding flow

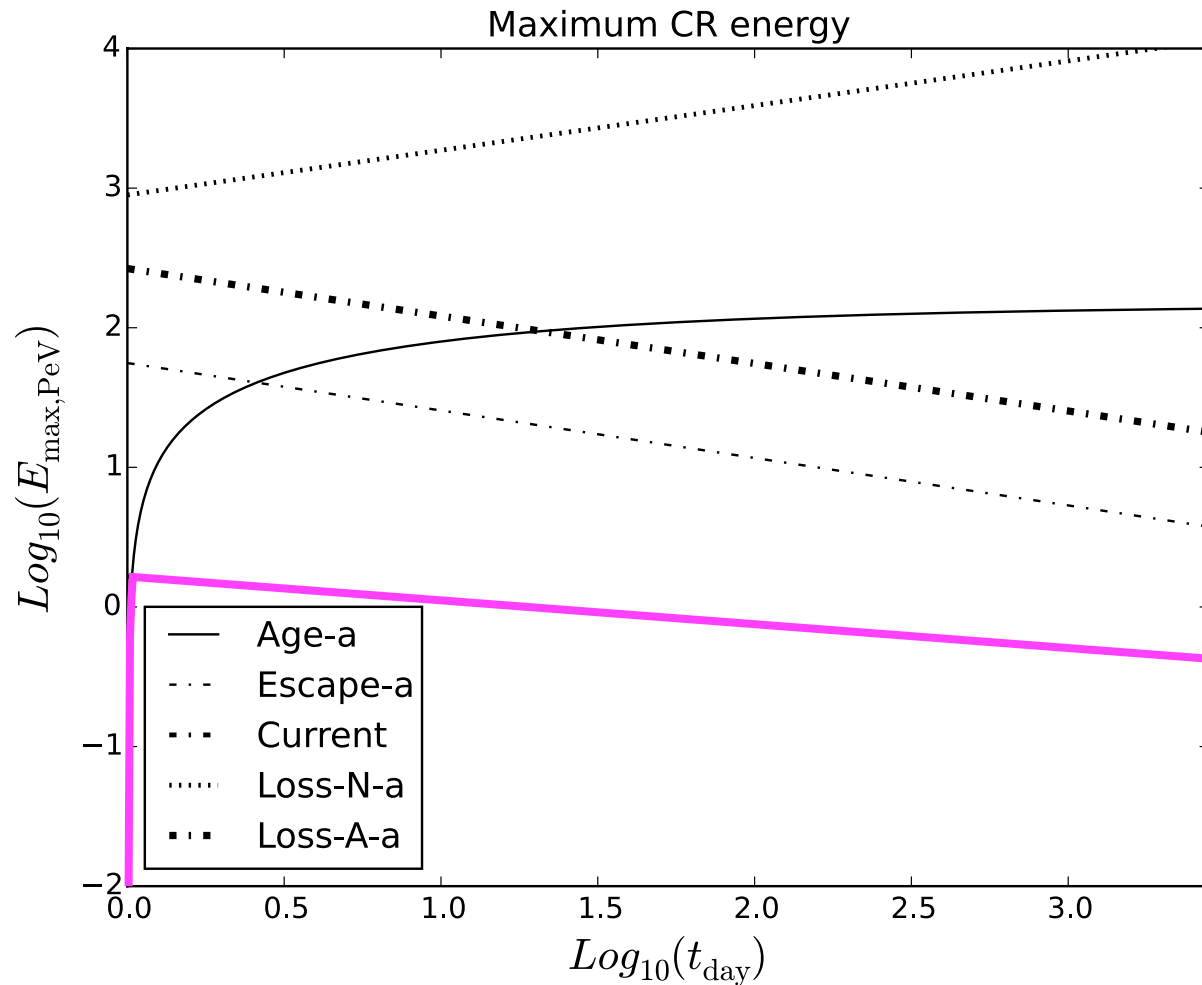
# Maximum Cosmic-Ray Energies



Maximum CR energy limits in PeV units for Parallel shock model as a function of time after shock breakout for SN 1993J. The background field has been amplified up to  $B_{\text{sat,NRS}}$ . The dotted line plots  $E_{\text{max,nuc}}(t)$ , the large dot-dashed line plots  $E_{\text{max,adi}}(t)$ , the intermediate dot-dashed line plots  $E_{\text{max,cur}}(t)$ , the small dot-dashed line plot  $E_{\text{max,esc}}(t)$ , the solid line plots  $E_{\text{max,age}}(t)$ . We use:  $\varpi = 1$ ,  $\eta = 1$ ,  $N = 5$ ,  $\phi = 14$ ,  $\sigma_{\text{pp}} = 1.87$ .




# Maximum Cosmic-Ray Energies



Maximum CR energy limits in PeV units for Parallel shock model as a function of time after shock breakout for SN 1993J. The background field has been amplified up to  $B_{\text{sat,NRS}}$ . The dotted line plots  $E_{\text{max,nuc}}(t)$ , the large dot-dashed line plots  $E_{\text{max,adi}}(t)$ , the intermediate dot-dashed line plots  $E_{\text{max,cur}}(t)$ , the small dot-dashed line plot  $E_{\text{max,esc}}(t)$ , the solid line plots  $E_{\text{max,age}}(t)$ . We use:  $\varpi = 1$ ,  $\eta = 1$ ,  $N = 5$ ,  $\phi = 14$ ,  $\sigma_{\text{pp}} = 1.87$ .

(Marcowith, VVD et al 2018, MNRAS, 479, 4470)

# Gamma-Ray Emission from Young SNe

- The SN shock expands with high velocity in these high density winds.
- Protons accelerated by the SN shock wave interact with protons in the surrounding medium, giving rise to hadronic  $\gamma$ -ray emission via pion decay.
- Hadronic emission depends on the proton density of the target material, and thus the density of the medium.
-  The hadronic emission will be highest where the density is the largest, i.e close-in to the star.
- The high radio emission from young SNe points to large magnetic fields.
- The combination of accelerated particles, large magnetic fields and high density indicates high gamma-ray emission.

(Marcowith, VVD et al 2018, MNRAS, 479, 4470)

# Gamma-rays from SNe

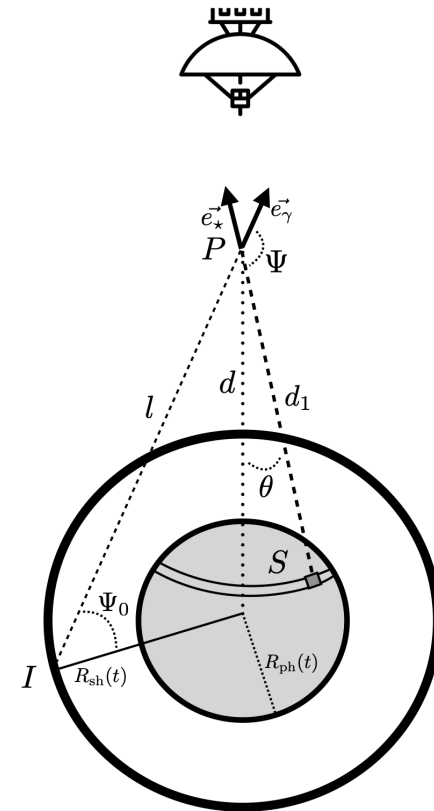
Gamma rays from particles accelerated at the shock

$$F_{\gamma}(> 1\text{TeV}) \approx 4.8 \times 10^{-14} \left(\frac{\xi_{\text{CR}}}{0.1}\right) \left(\frac{\dot{M}_w}{10^{-6} M_{\odot}/\text{yr}}\right)^2 \left(\frac{v_w}{10^6 \text{ cm/s}}\right)^{-2} \left(\frac{D}{\text{Mpc}}\right)^{-2} \left(\frac{v_{\text{sh}}(t)}{10^9 \text{ cm/s}}\right)^2 \left(\frac{R_{\text{sh}}(t)}{10^{14} \text{ cm}}\right)^{-1} \text{ cm}^{-2} \text{ s}^{-1}$$

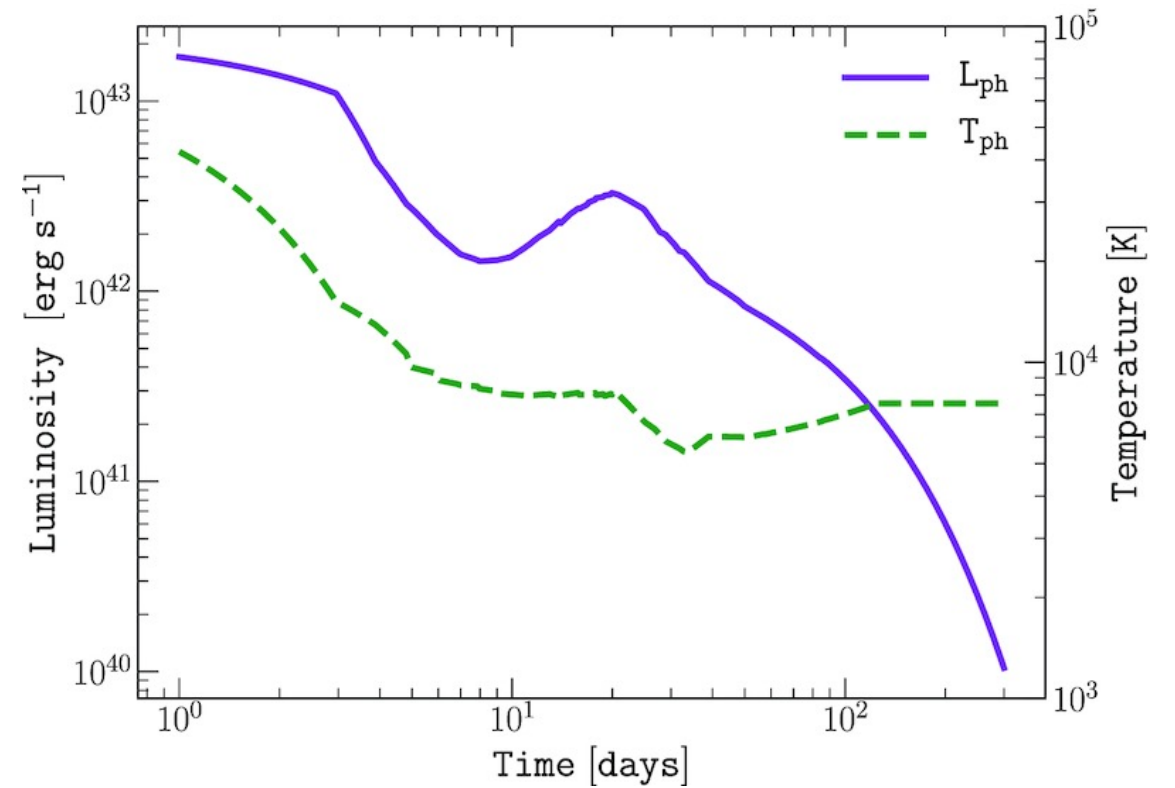
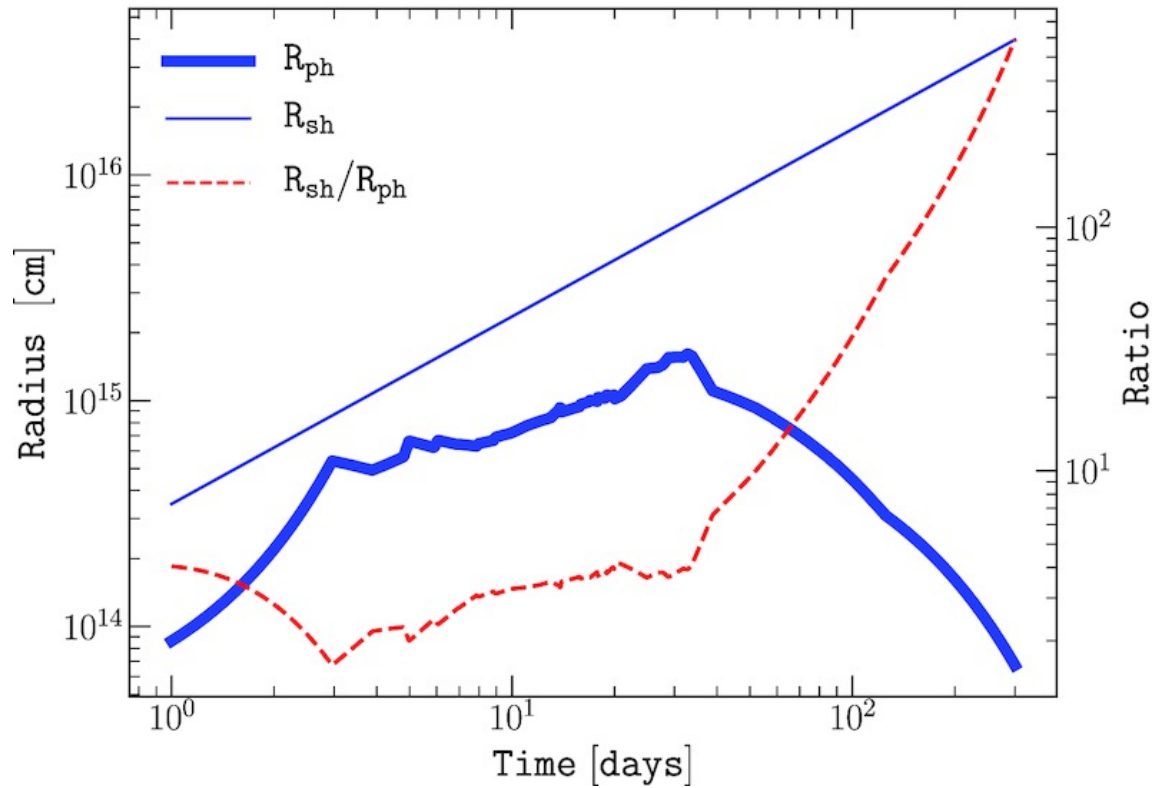
Degraded by pair production:

$$\gamma\gamma \rightarrow e^+e^-$$

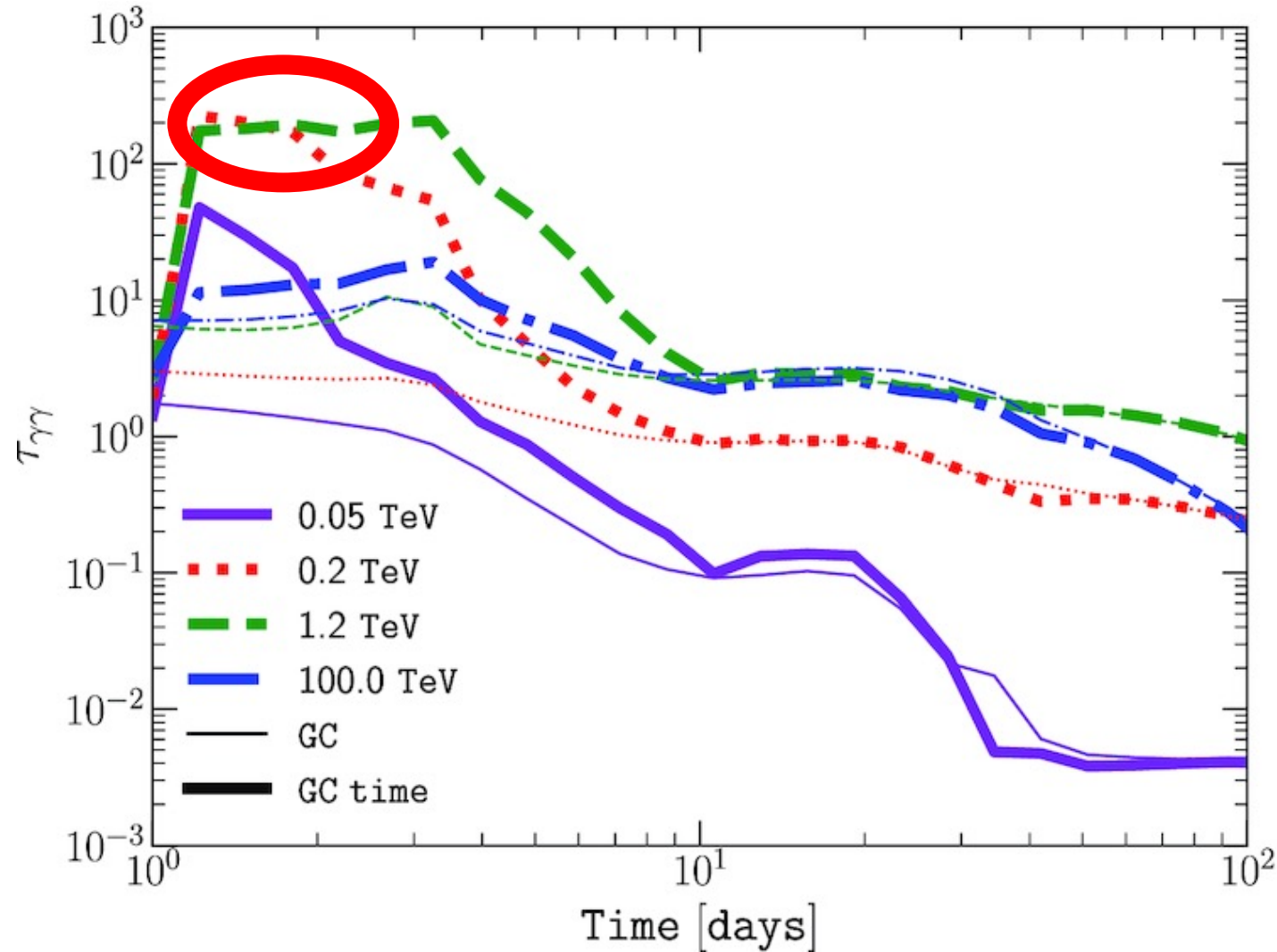
$$\tau_{\gamma\gamma}(E) = \int_0^t dt' \int_{\psi_{0,\min}}^{\pi} d\psi_0 \int_0^{+\infty} dl \int_{c_{\min}}^1 d \cos \theta \int_0^{2\pi} d\phi \int_{\epsilon_{\min}}^{+\infty} d\epsilon \frac{d\tau_{\gamma\gamma}}{d\epsilon d\Omega dl}$$



# Gamma-Gamma Absorption in SN 1993J: What we need



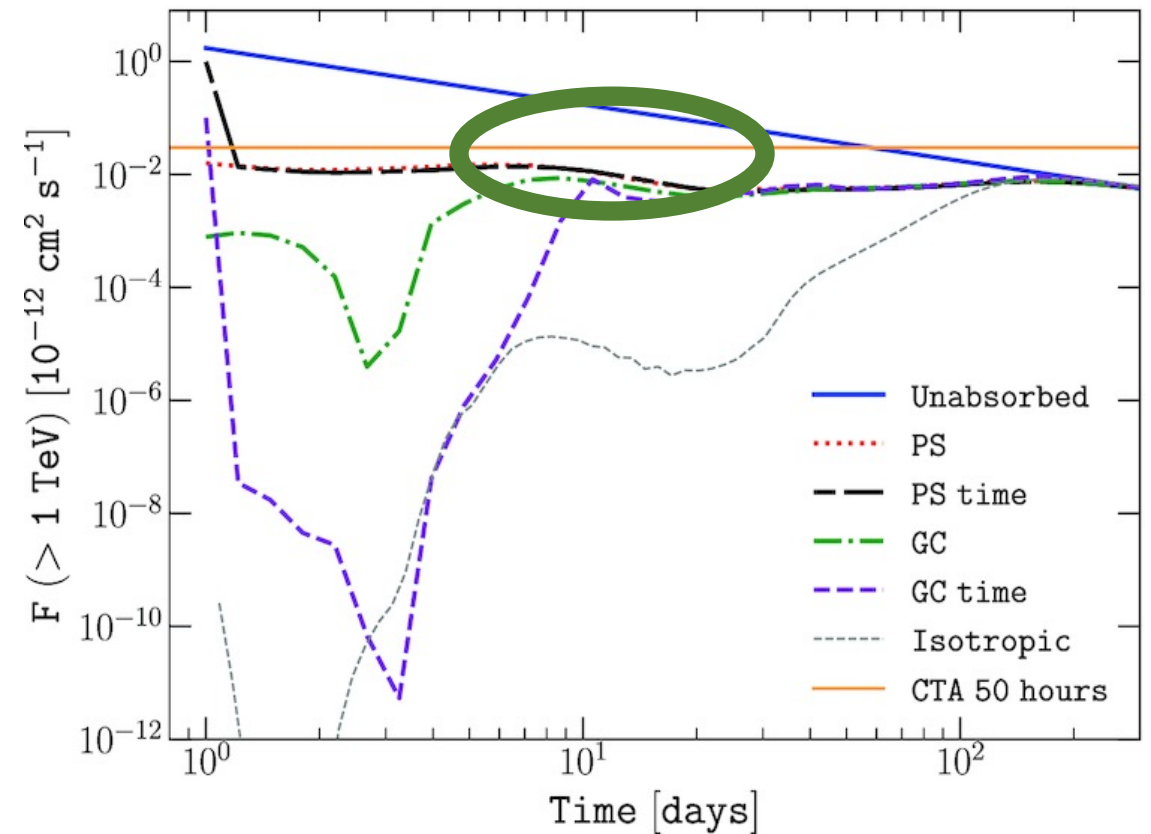
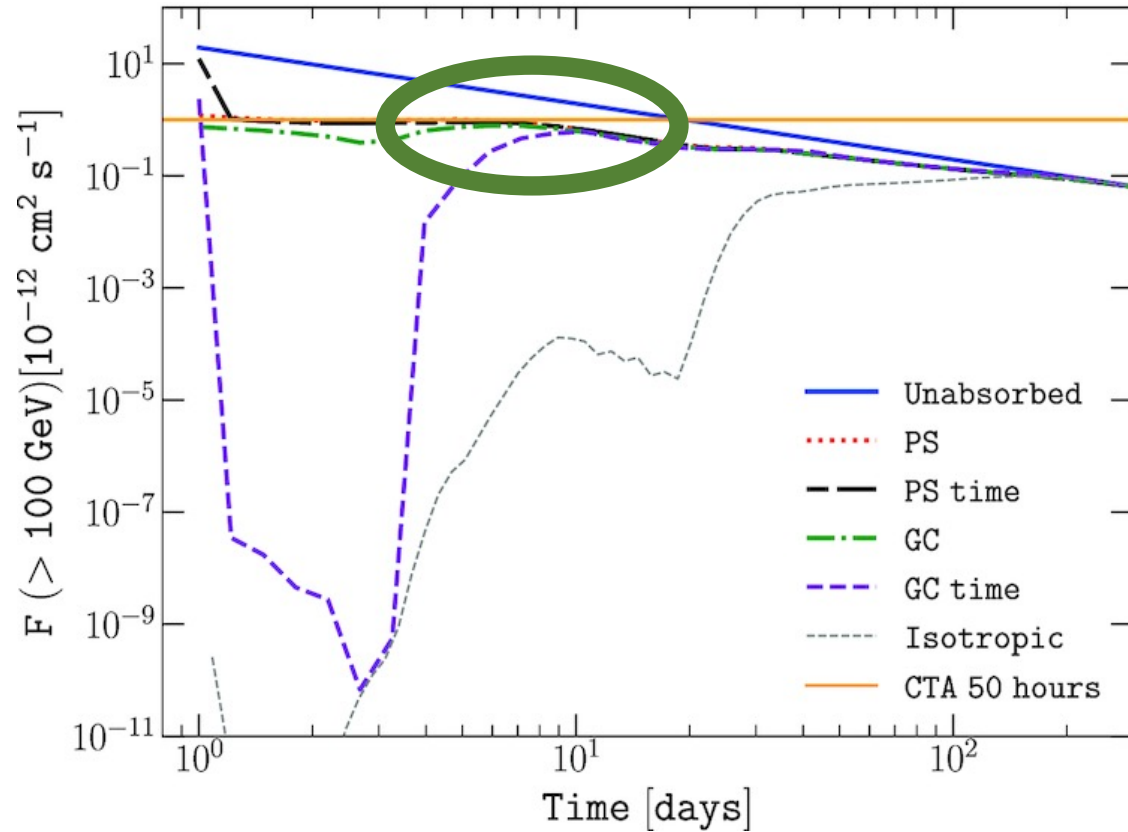
# Gamma-gamma absorption



Time evolution of the opacity  $\tau_{\gamma\gamma}$  for gamma-rays of different energies. The general cases with temporal effects (GC time, thick lines) and without temporal effects (GC, thin lines) are shown.

Cristofari, Marcowith, Renaud, VVD, Tatischeff, MNRAS, 2020, 494, 2760

# Gamma-gamma absorption



Time evolution of the integrated flux above 100 GeV from SN 1993J. Six cases are shown: unabsorbed (blue solid), point source (PS, red dotted), point source with time effects (PS time, black dot long dashed), general case (GC, green dot dashed), general case with time effects (GC time, purple dashed), and the isotropic calculation (grey thin dotted) (Aharonian et al. 2008). The typical sensitivity of CTA in 50 h at energies above 100 GeV (Fioretti, Bulgarelli & Schüssler 2016) is shown as the horizontal orange line.

Time evolution of the integrated flux over 1 TeV from SN 1993J

Cristofari, Marcowith, Renaud, VVD, Tatischeff, MNRAS, 2020, 494, 2760

# Type IIP SNe

Most frequent type of SNe  
 Helpful for description of  
 other types

## Shock dynamics

$$R_{\text{sh}}(t) \approx 4.7 \times 10^{14} \left( \frac{E_{\text{SN}}}{10^{51} \text{ erg}} \right)^{0.44} \left( \frac{\dot{M}_w}{10^{-6} M_{\odot}/\text{yr}} \right)^{-0.17} \left( \frac{M_{\text{ej}}}{M_{\odot}} \right)^{-0.31} \left( \frac{t}{\text{days}} \right)^{0.875} \text{ cm}$$

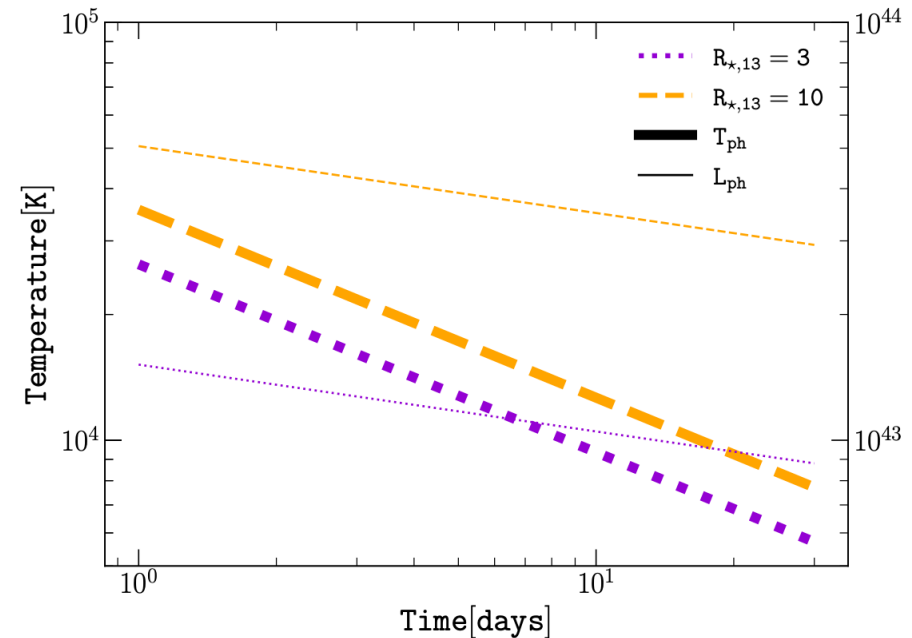
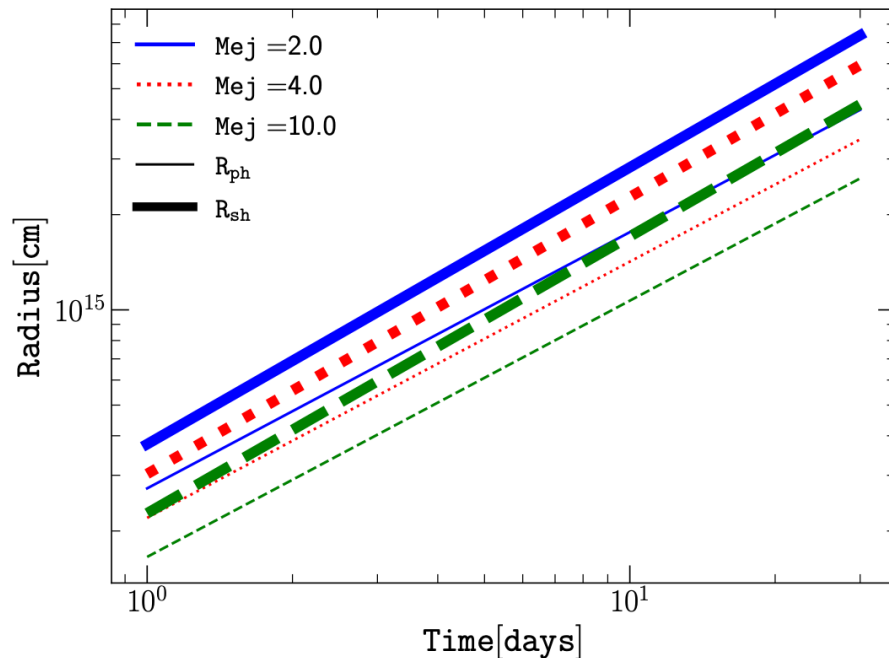
Chevalier 1999

## Photosphere

$$r_{\text{ph}}(t) = 2.9 \times 10^{14} \left( \frac{f}{0.1} \right)^{-0.062} \left( \frac{E_{\text{SN}}}{10^{51} \text{ erg}} \right)^{0.41} \left( \frac{\kappa}{0.34} \right)^{0.093} \left( \frac{M_{\text{ej}}}{M_{\odot}} \right)^{-0.28} \left( \frac{t}{\text{days}} \right)^{0.81}$$

Rabinak 2011

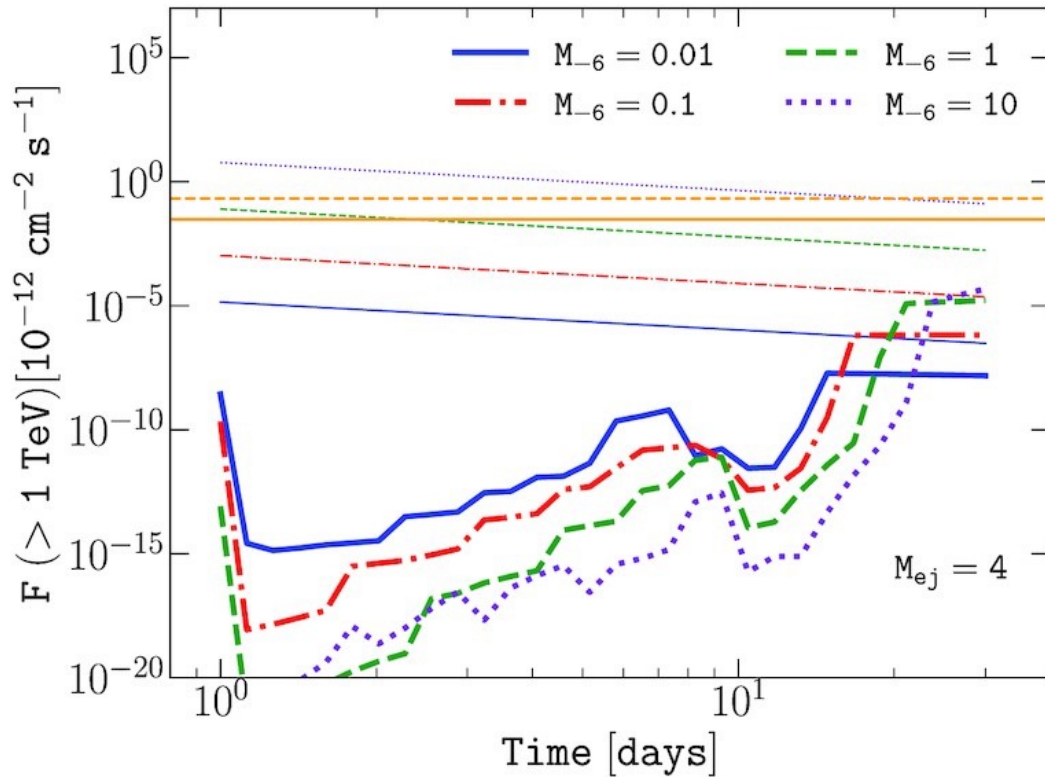
$$T_{\text{ph}}(t) = 1.7 \left( \frac{f}{0.1} \right)^{-0.037} \left( \frac{E_{\text{SN}}}{10^{51} \text{ erg}} \right)^{0.027} \left( \frac{R_{\star}}{10^{13} \text{ cm}} \right)^{1/4} \left( \frac{M_{\text{ej}}}{M_{\odot}} \right)^{-0.054} \left( \frac{\kappa}{0.34 \text{ cm}^2/\text{g}} \right)^{-0.28} \left( \frac{t}{\text{days}} \right)^{-0.45} \text{ eV}$$



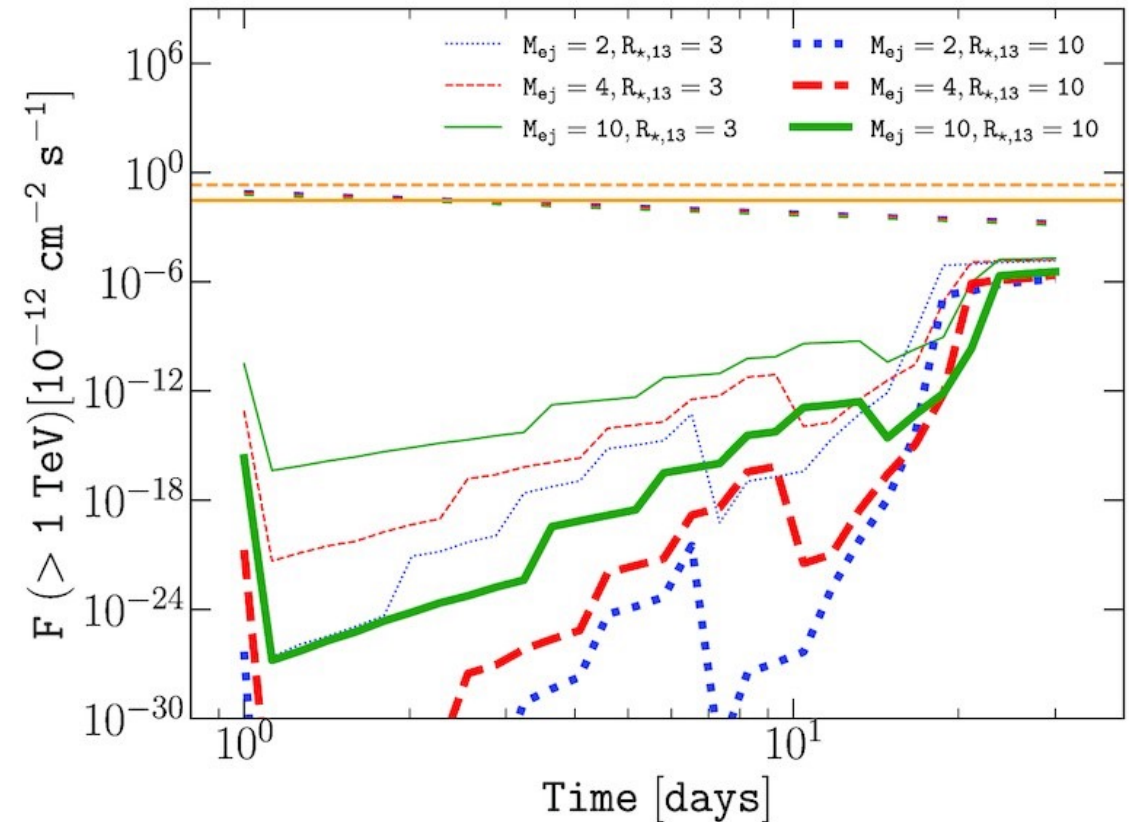


# Type IIP SNe

Cristofari, Marcowith, Renaud, VVD, et al. 2022,  
MNRAS, 511, 3321

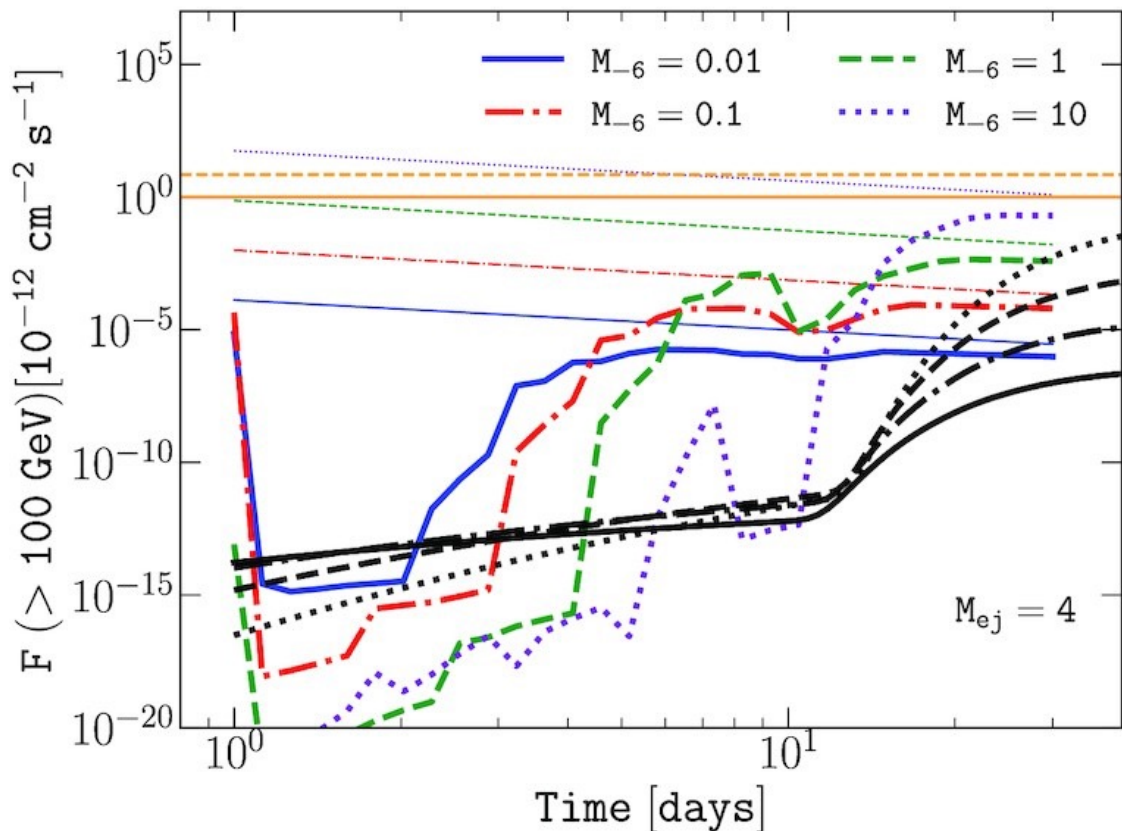


Time evolution of the integrated photon flux above 1 TeV. The source distance is  $D = 1 \text{ Mpc}$ , the ejecta mass is  $M_{ej} = 4 M_{\odot}$ , the progenitor radius is  $R_{\star} = 3 \times 10^{13} \text{ cm}$ . The mass-loss rate of the wind  $10^{-8}$ ,  $10^{-7}$ ,  $10^{-6}$ , and  $10^{-5} M_{\odot} \text{ yr}^{-1}$ , is shown as solid (blue), dot-dashed (red), dashed (green), and dotted (violet) lines, respectively. The corresponding unattenuated fluxes are shown as thin lines. The typical sensitivity of CTA for 50 h (solid orange horizontal line) and 2 h (dashed orange horizontal line) is shown as a guiding-eye for the reader

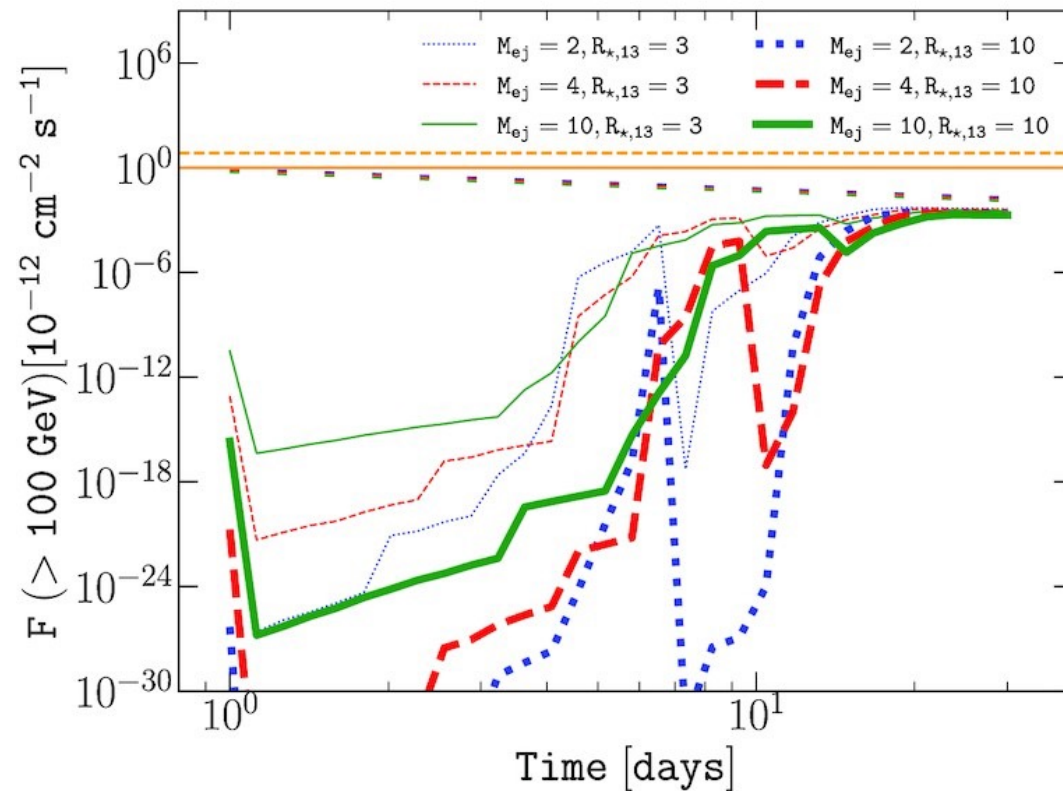




# Type IIP SNe



Time evolution of the integrated photon flux above 100 GeV. The source distance is  $D = 1$  Mpc, the ejecta mass is  $M_{ej} = 4 M_{\odot}$ , the progenitor radius is  $R_{\star} = 3 \times 10^{13}$  cm. The mass-loss rate of the wind  $10^{-8}$ ,  $10^{-7}$ ,  $10^{-6}$ , and  $10^{-5} M_{\odot} \text{ yr}^{-1}$ , is shown as solid (blue), dot-dashed (red), dashed (green), and dotted (violet) lines, respectively. The corresponding unattenuated fluxes are shown as thin lines. The typical sensitivity of CTA for 50 h (solid orange horizontal line) and 2 h (dashed orange horizontal line) is shown as a guiding-eye for the reader



# Type II<sub>n</sub> « interaction powered SNe »: SN2005ip, SN2006jd, SN2010jl

Bolometric light and gamma rays powered by the interaction between SN ejecta and dense CSM.

SN	$s (\rho_{\text{CSM}} \propto r^{-s})$		$\langle \dot{M} \rangle^a$ ( $M_{\odot} \text{ yr}^{-1}$ )	$E_{\text{ej}}$ ( $10^{51} \text{ erg}$ )
	$n = 10$	$n = 12$		
2005ip	2.3	2.4	$1.2\text{--}1.4 \times 10^{-3}$	$13\text{--}15^b$
2006jd	1.4	1.6	$1.3\text{--}1.7 \times 10^{-3}$	$12\text{--}13^b$
2010jl		$2.2^b$	$0.039^b$	$23^b$

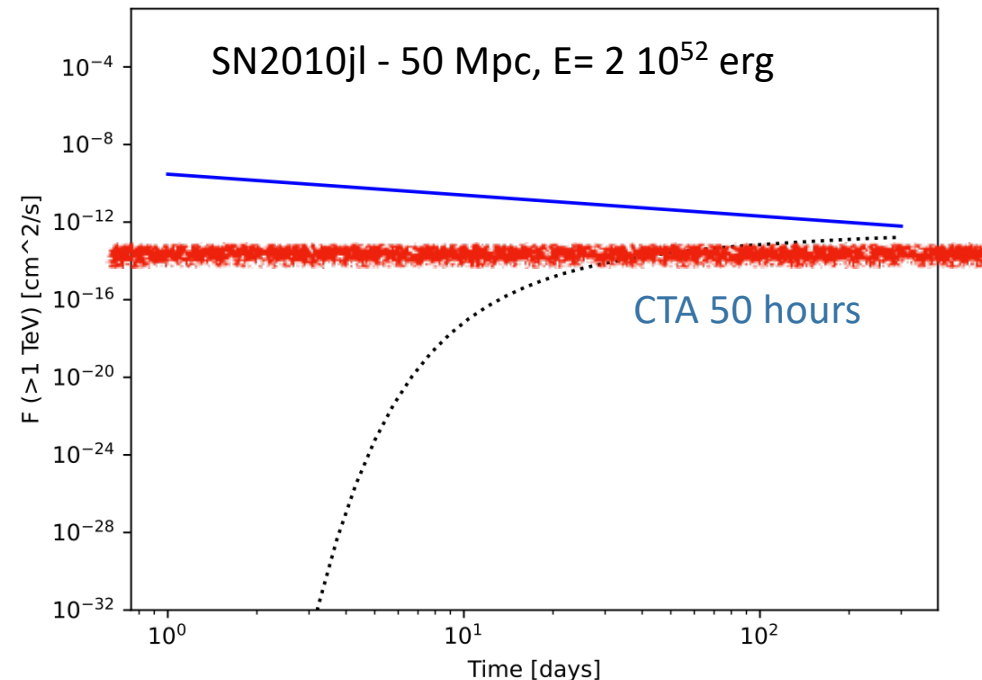
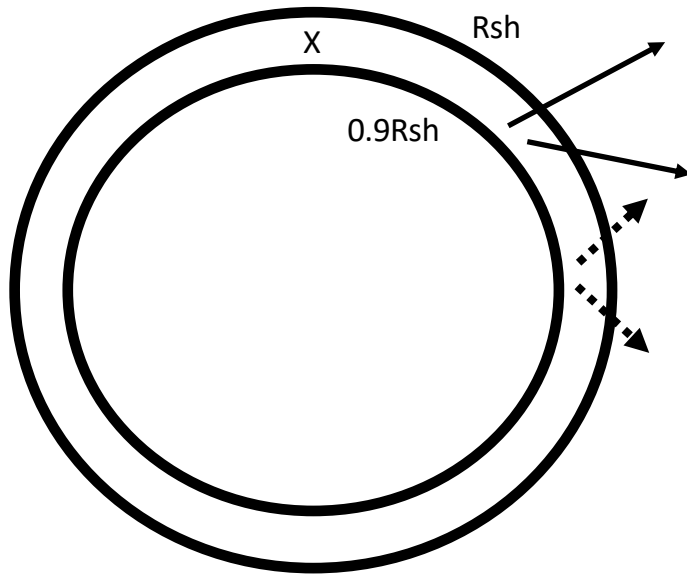
<sup>a</sup> Average rate derived by the CSM mass within  $10^{16}$  cm and the CSM wind velocity  $100 \text{ km s}^{-1}$ .

<sup>b</sup> Derived assuming  $M_{\text{ej}} = 10 M_{\odot}$ .

Very large values

# Type IIIn « interaction powered SNe »: SN2005ip, SN2006jd, SN2010jl

Simplified picture: gamma rays and soft photons from the same shell: « isotropic-like » calculation - Work in progress



Radiative shocks? Particle acceleration? Spectrum? Efficiency?

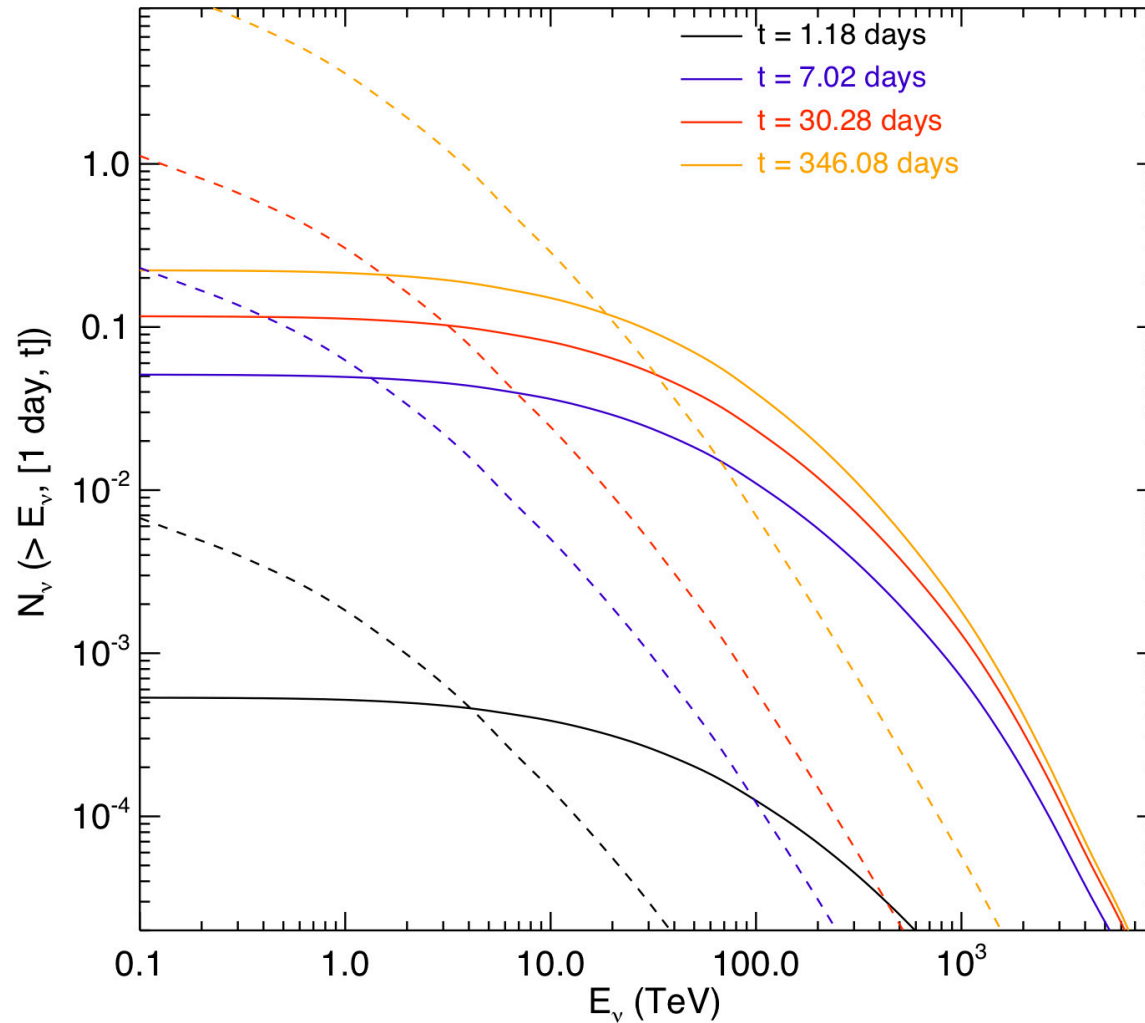
# Conclusions

- Highest GCR energies are reached for **fast shocks**. Current driven instabilities grow the fastest in **dense environments**.
- SN 1993J:
  - **Maximum energies: Up to few PeV** for protons,
  - **Gamma-gamma absorption reduces flux considerably.**
  - Gamma-ray detection of 93J-like SNe possible above 0.1TeV for CTA. Much higher ambient densities required for HESS, VERITAS, MAGIC.
  - High-energy neutrinos expected however the flux is low (depends on p-p interaction and surrounding density).
- Other SN classes:
  - **Type IIP SNe** are the most numerous, but do not seem viable candidates above 100 GeV unless we find one close by (< 1 Mpc).
  - **Type IIn** seem obvious targets – high density in surrounding medium. Absorption can last for hundreds of days. Work still in progress.

**CTA will depend on astronomers at other wavelengths (optical, radio, Xray) to ascertain the type of SN and the SN parameters, in order to define the observing program for any given SN.**

# Questions and Discussions

# Neutrinos



Neutrinos are by-products of pion production. Time dependent neutrino flux of SN 1993J above an energy  $E$  expected by an instrument equivalent to KM3NeT (solid lines) at four different times after the outburst. Dotted lines show the atmospheric neutrino backgrounds. In order to detect at least one neutrino from such a source, it must be at a distance  $< 1$  Mpc, or the gamma-ray signal has to be ten times stronger.